Supporting Information

Single Layer Graphene Encapsulating Non-Precious Metals as High-performance Electrocatalysts for Water Oxidation

Xiaoju Cui[‡], Pengju Ren[‡], Dehui Deng[*], Jiao Deng, Xinhe Bao[*]

State Key Laboratory of Catalysis, *i*ChEM, Dalian Institute of Chemical Physics, Chinese Academy of Sciences, Zhongshan Road 457, Dalian, 116023, China.

[‡]These authors have contributed equally.

[*]E-mail: dhdeng@dicp.ac.cn; xhbao@dicp.ac.cn; Fax: +86-411-84694447;Tel: +86-411-84686637

Experimental section

Materials preparation

All the chemicals were commercial materials of analytical grade and received without further purification. The M@NCs (M represents Fe, Co, Ni, FeCo, FeNi and CoNi) were prepared through a chemical vapor deposition (CVD) method. In a typical approach, firstly, 3.6 mmol metal-containing precursors, i.e. $Fe(NO_3)_3 \cdot 9H_2O$, $Co(NO_3)_2 \cdot 6H_2O$, $Ni(NO_3)_2 \cdot 6H_2O$ or their mixture (two kinds of metal-containing precursors molar ratio of 1:1) were filled into the channel of 1.0 g SBA-15 by an impregnation method in 50 mL methanol solution. Then the catalysts were transferred into a CVD furnace, temperature programmed from room temperature to 700 ^oC under 50% H_2/Ar, followed by bubbling CH_3CN with 80 mL min^{-1} Ar for 20 minutes at 700 ^oC. Finally, the samples were treated in 4% HF aqueous solution at room temperature for 8 h, followed by washing in distilled water and ethanol, and then drying at 100 ^oC for 12 h. The resulting samples were denoted as Fe@NC, Co@NC, Ni@NC, FeCo@NC, FeNi@NC and CoNi@NC, respectively according to the types of the metal precursors. FeNi@C was prepared in the same way except using C_2H_4 instead of CH_3CN as carbon source. N-FeNi@C was prepared as the same procedure of FeNi@C except using the mixture of C_2H_4 and NH_3 instead of pure C_2H_4. The carbon nanotubes (CNTs) were purchased from Chengdu Organic Chemicals Co. Ltd. CAS, which were further treated by refluxing in concentrated HNO_3 under 130 ^oC for 12 h to remove the impurities. The few-layer graphene was prepared according to the ball milling process reported by our previous work[1]. The N-graphene, N-CNTs and N-graphite oxide (N-GO) was obtained via treating the few-layer graphene, CNTs and graphite oxide in NH_3 under 700 ^oC for 2 h.

Materials characterization

Scanning electron microscopy (SEM) and scanning transmission electron microscopy (STEM) were conducted on Hitachi S5500 operated at 30 kV. High resolution

transmission electron microscopy were conducted on a FEI Tecnai F30 microscope operated at an accelerating voltage of 300 kV and FEI Tecnai F20 microscope operated at an accelerating voltage of 200 kV. X-ray diffraction (XRD) was performed on a Rigaku D/Max-2500 diffractometer with Cu Kα radiation (λ=1.5418 Å) at 40 kV and 200 mA at a scan rate of 5^{o} min^{-1}. Raman spectroscopy was conducted on a Jobin Yvon LabRAM HR 800 instrument with a 532 nm excitation laser at a power of around 0.8 mW. X-ray photoelectron spectroscopy (XPS) was carried out on a VG ESCALAB MK2 spectroscope used Al Kα X-rays as the excitation source with a voltage of 12.5 kV and power of 250 W. Inductively coupled plasma atomic emission spectroscopy (ICP-AES) was carried out in SHIMADZU ICPS-8100 and the samples for ICP-AES analysis were first heated at 800 ^{o}C for 5 h in air, followed by treatment in concentrated hydrochloric acid at 110 ^{o}C for 12 h. The BET surface area of the proposed electrocatalysts were tested on TriStar II 3020 V1.03. The surface composition of C, N, H were determined by Vario EL III instrument.

Electrochemical measurements

Electrochemical measurements were performed on a 2273 potentiostat/galvanostat with a three-electrode electrochemical cell equipped with a gas flow controlling system. A commercial glassy carbon (GC) electrode (5 mm in diameter, 0.196 cm^2) covered by the sample with Nafion ionomer as a binder, Pt wire and Hg/HgO (1 M NaOH solution) in 1 M NaOH solution were used as the working electrode, counter electrode and reference electrode, respectively. Typically, 5 mg catalyst was dispersed in 2 mL ethanol with 50 μL Nafion solution (5 wt.%, Du Pont) to form homogeneous ink assisted by ultrasound. Then 25 μL of the ink was added dropwise onto the surface of GC using a micropipette and dried under room temperature. The final loading for all catalysts and commercial IrO_2 on working electrode is 0.32 mg/cm^2. The OER activities of different samples were evaluated by roating disk electrode (RDE) measurements in O_2 saturated 1 M NaOH electrolyte at 25 ^{o}C with a scan rate

of 5 mV s^{-1}. Before the OER test, the samples were repeatedly swept from -0.5 V to 0 V in O_2-saturated 1 M NaOH solution until a steady voltammogram curve was obtained.

DFT calculation method

Vienna Ab-initio Simulation Package (VASP)[2-5] was used for all calculations with Perdew-Burke-Ernzerhof (PBE) functional[6, 7] for the exchange-correlation term and the projector augmented wave method[8, 9]. The cutoff energies for all calculations were set to 400 eV. The models of metal particles encapsulated into graphene layer (M@Cs) consist of C_{240} encapsulating 55 atoms metal cluster, such as Fe, Co, Ni and their alloys etc. All structures were fully relaxed to the ground state and spin-polarization was considered in all calculations. The convergences of energy and force were set to 1×10^{-4} eV and 0.05eV/Å, respectively. The free energies of the intermediates at 298.15 K were obtained by $\Delta G = \Delta E + \Delta ZPE - T\Delta S + eU$, where ΔE is the binding energy of adsorption species HO*, O* and HOO*, ΔZPE, ΔS and U are the zero point energy changes, entropy changes and applied potentials, respectively. The contributions of each component for ΔG were obtained according to the approach by Rossmeisl et al.[10] and were listed in Table S6. The data for IrO_2 is obtained from Rossmeisl et al. in Fig 3c for comparison.

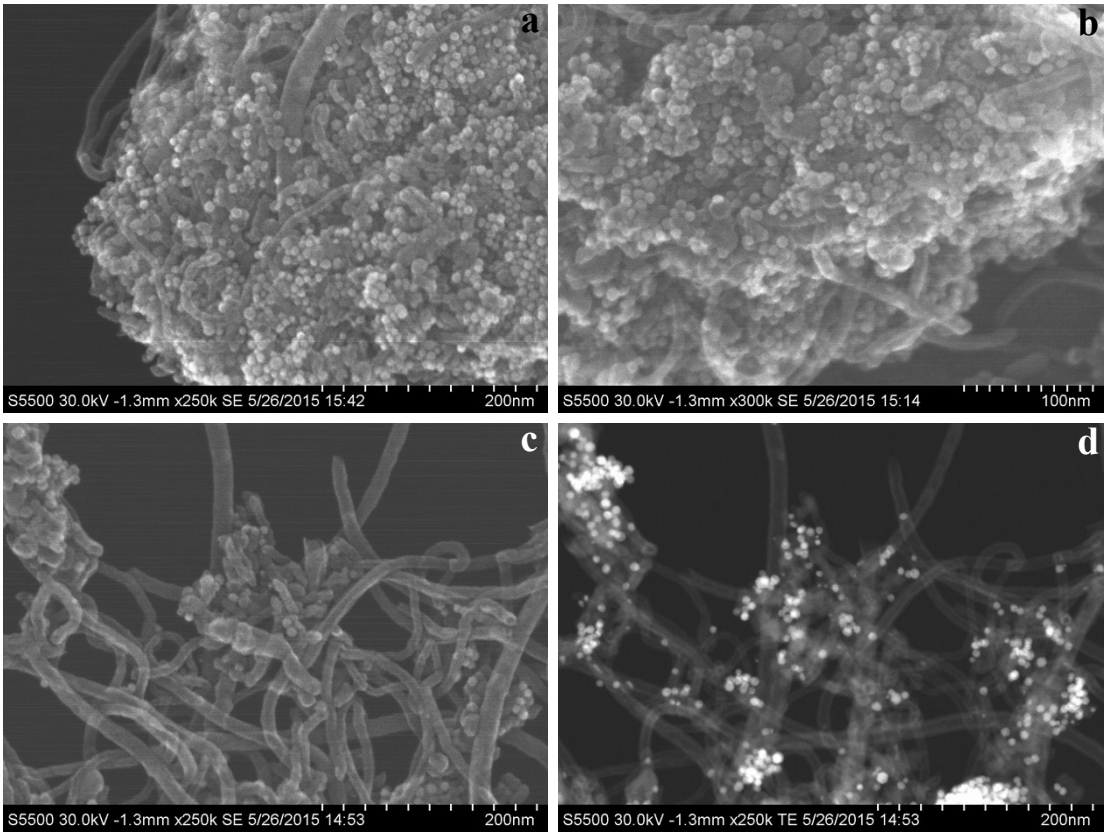

Fig S1. (a-c) SEM images of FeNi@NC, (d) The STEM image of FeNi@NC in the same region with SEM image of (c).

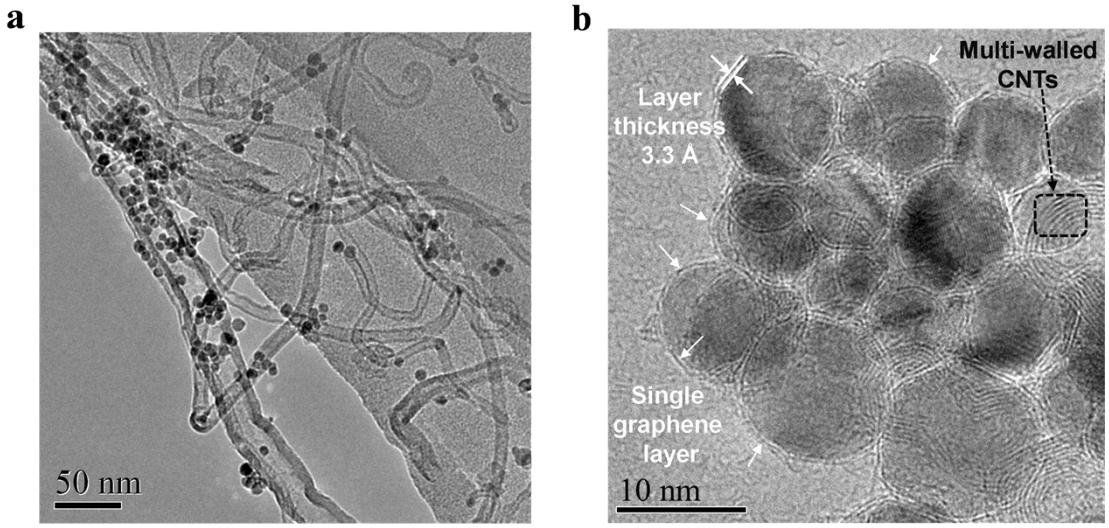

Figure S2. (HR) TEM images of FeNi@NC.The white arrows represent the single layer graphene and the black arrow represents the multi-walled CNTs.

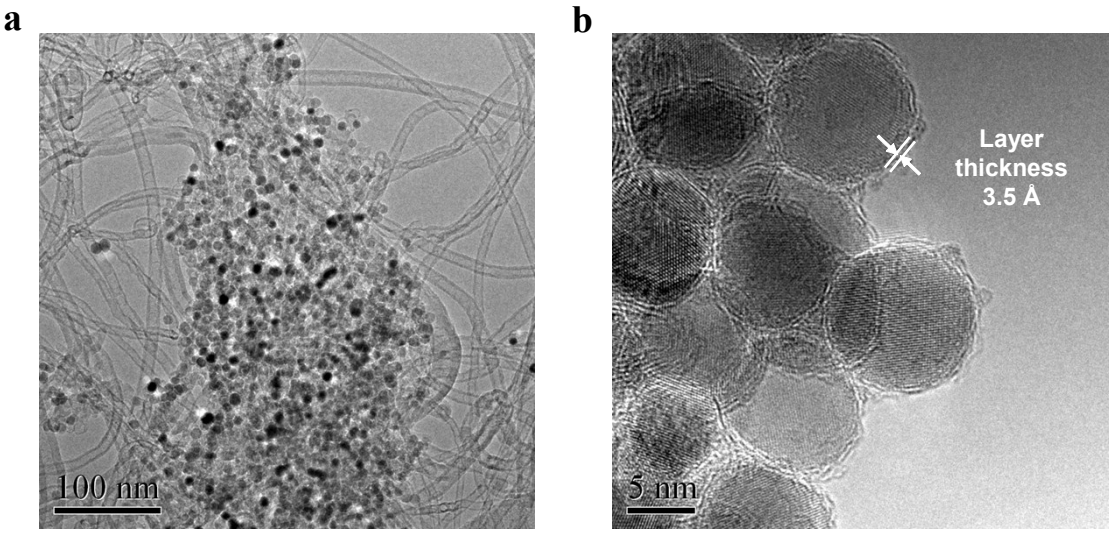

Figure S3. (HR) TEM images of Fe@NC.

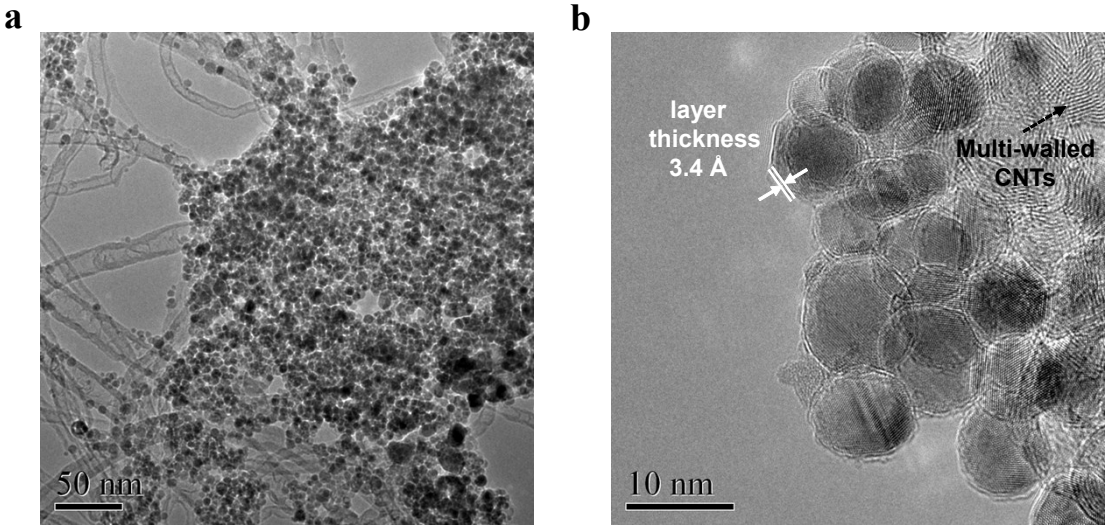

Figure S4. (HR) TEM images of Co@NC.

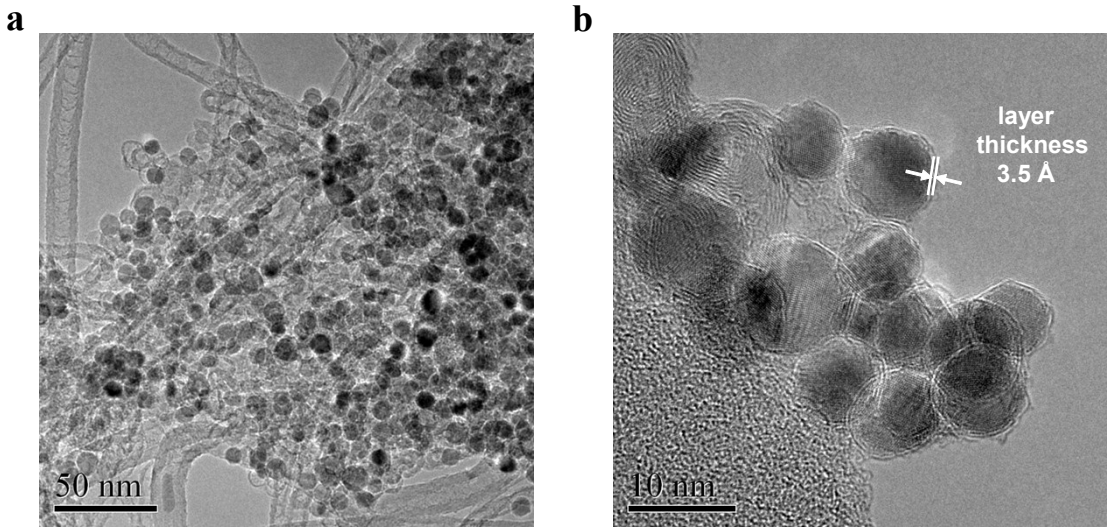

Figure S5. (HR) TEM images of Ni@NC.

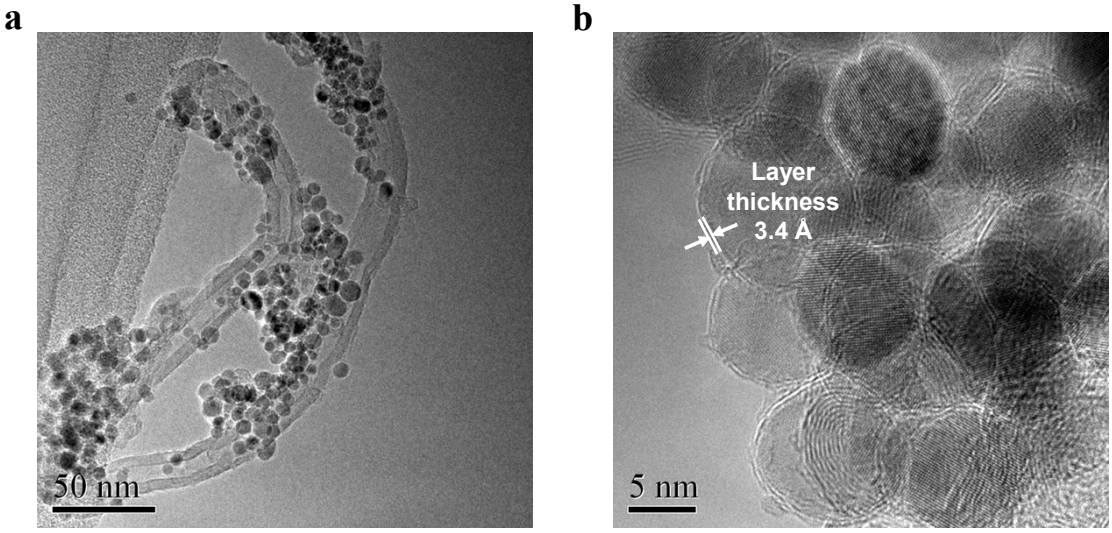

Figure S6. (HR) TEM images of FeCo@NC.

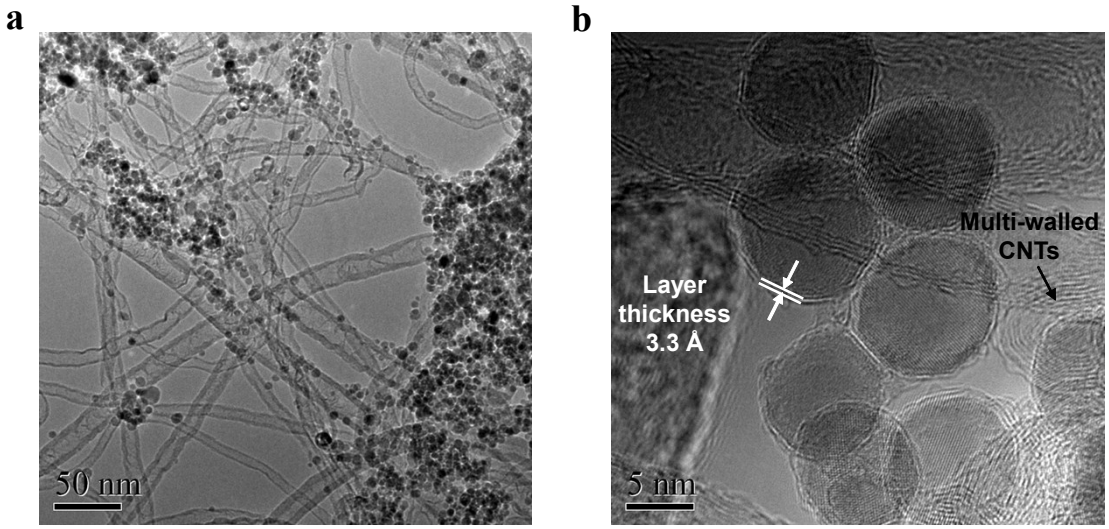

Figure S7. (HR) TEM images of CoNi@NC.

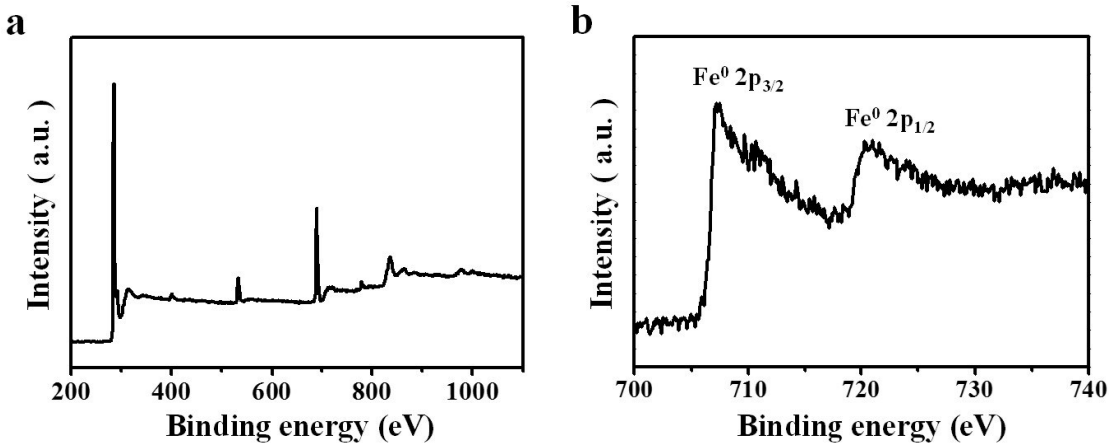

Figure S8. XPS spectra of Fe@NC: (a) wide XPS, (b) Fe 2p spectra.

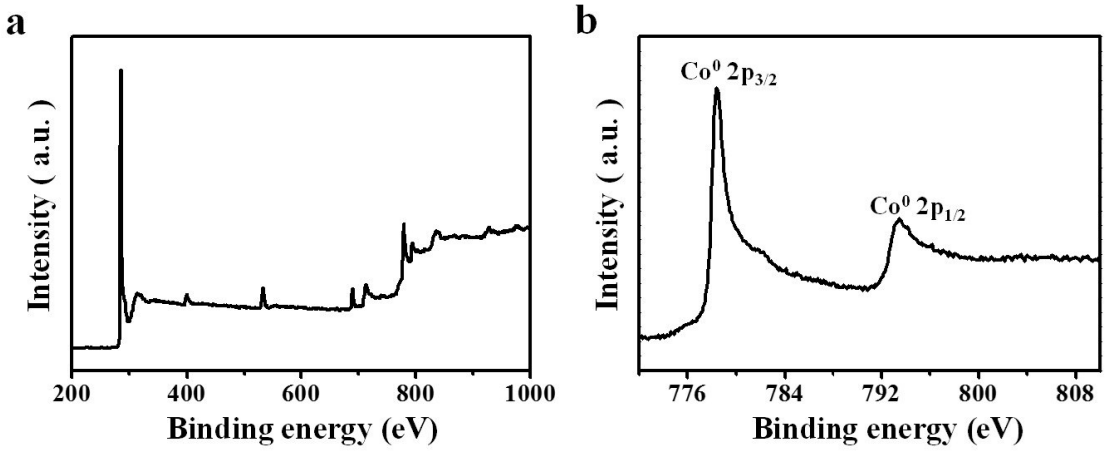

Figure S9. XPS spectra of Co@NC: (a) wide XPS, (b) Co 2p spectra.

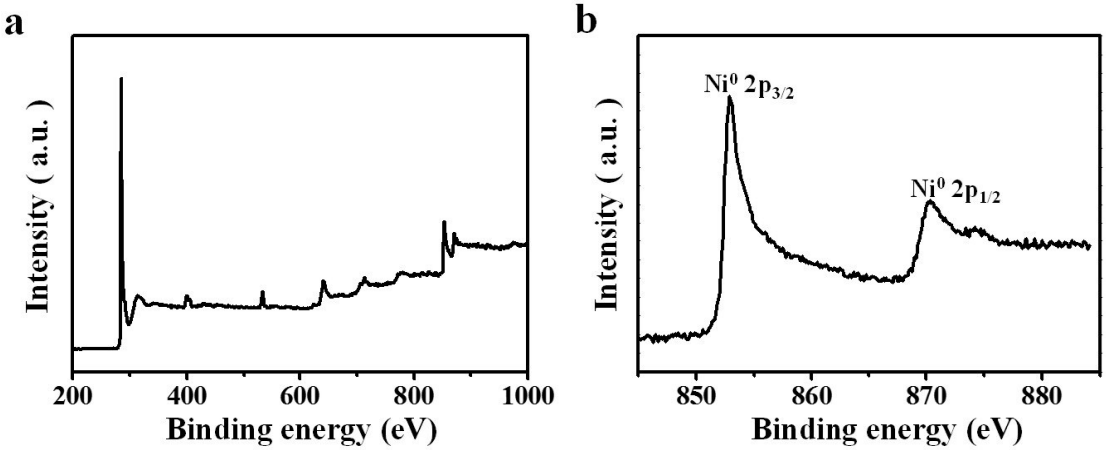

Figure S10. XPS spectra of Ni@NC: (a) wide XPS, (b) Ni 2p spectra.

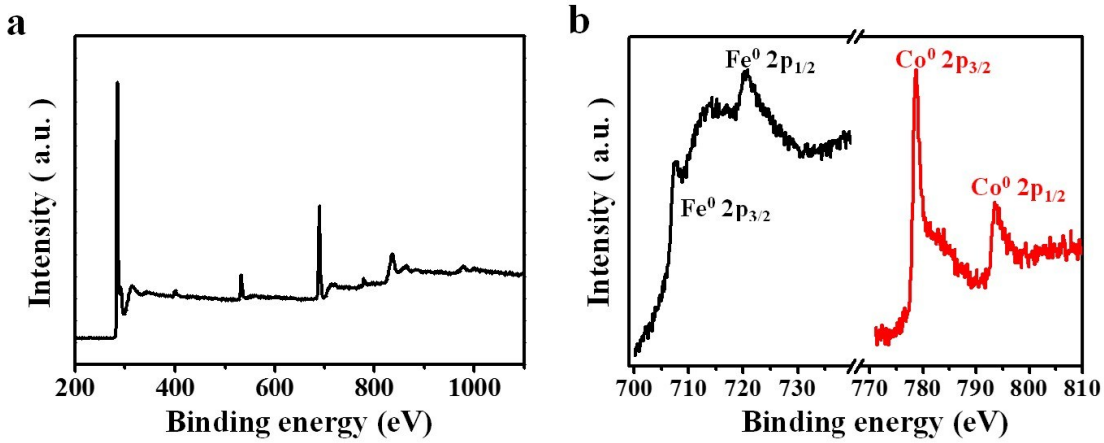

Figure S11. XPS spectra of FeCo@NC: (a) wide XPS, (b) Fe 2p and Co 2p spectra.

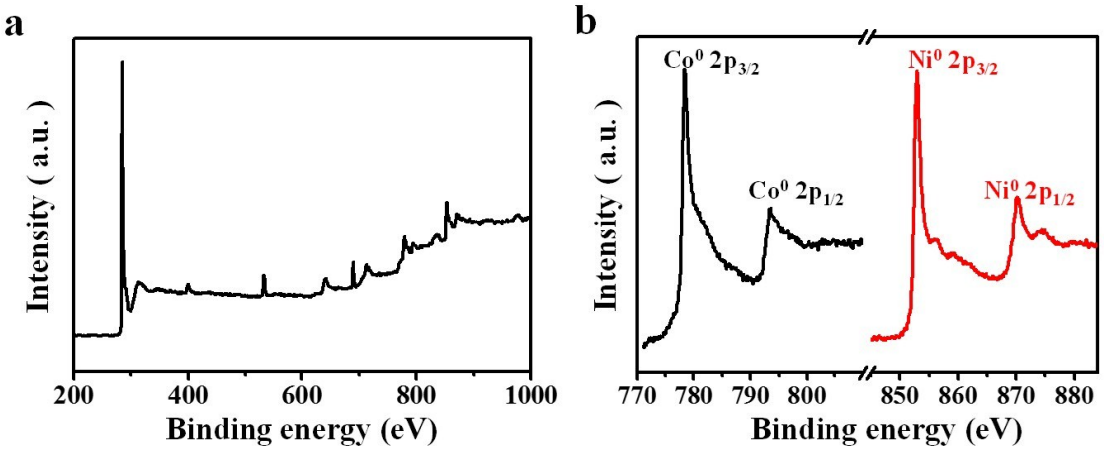

Figure S12. XPS spectra of CoNi@NC: (a) wide XPS, (b) Co 2p and Ni 2p spectra.

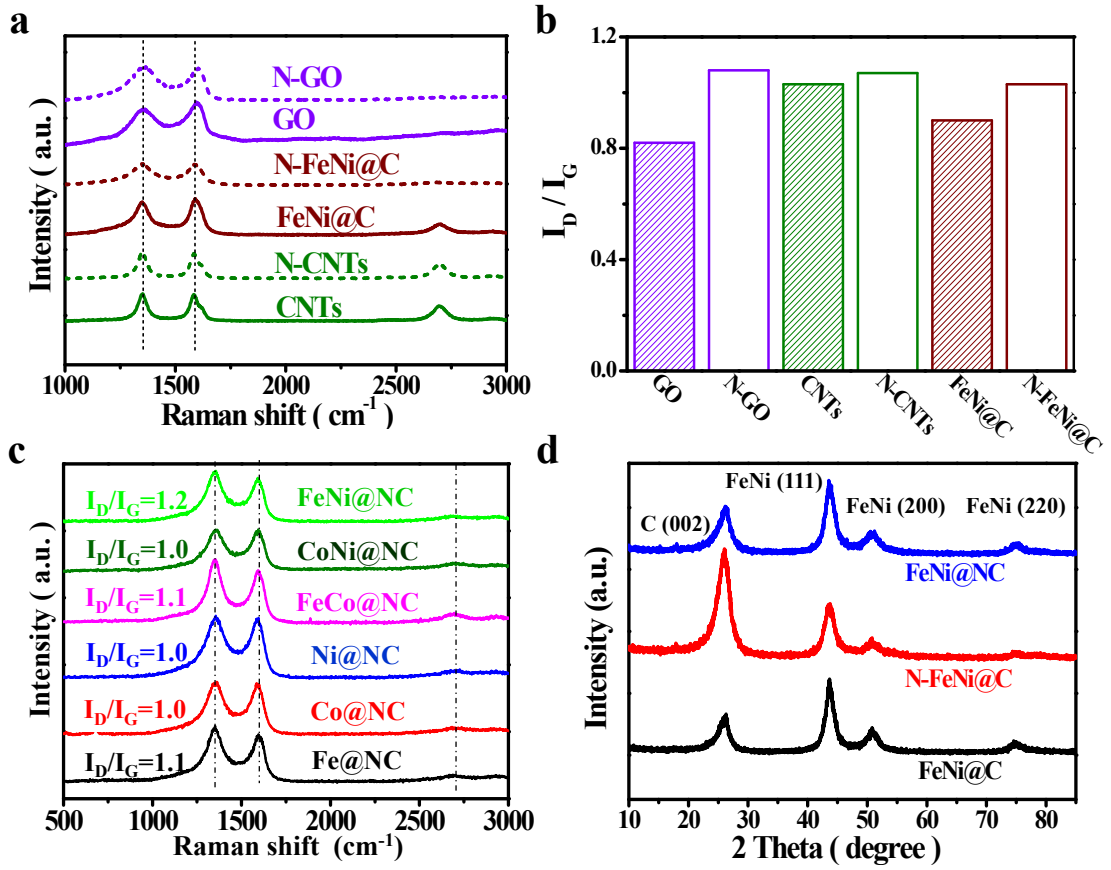

Figure S13. (a)-(c) Raman spectra and the corresponding intensity ratio of D peak and G peak (I_D/I_G) of M@NCs, N doped C and C samples. **(d)** XRD patterns of FeNi@NC, FeNi@C and N-FeNi@C samples.

M@NCs were composites of single layer graphene encapsulating metal nanoparticles and a small quantity of multi-walled carbon nanotubes. In which, the graphene layers in our samples include some N dopants, which can increase the I_D/I_G ratio as reported by the reference (J. Appl. Phys., 2014, 116, 233101). In addition, it is demonstrated that the substrate-graphene interaction can change the microstructure and the band structure of the graphene (J. Phys. Chem. C., 2012, 116, 4732), which may increase the D peak intensity, and therefore when the metal was encapsulated by graphene, the interaction between graphene layer and encapsulated metal could increase the I_D/I_G ratio. So, the relatively high I_D/I_G ratio of the M@NCs was probably due to the N doping, the direct interaction between graphene layer and encapsulated metal, and also some possible defects at the cages and CNTs in the samples.

The interaction between graphene and encapsulated metal could alter the

graphene lattice structure and decrease the 2D peak intensity as reported by J. Phys. Chem. C., 2012, 116, 4732. Besides, the N doping can shift the Fermi level away from the Dirac point, and decrease the intensity of the 2D peak as reported by Mod. Phys. Lett. B., 2011, 25, 511. In addition, the multi-walled carbon nanotubes in these samples can also decrease the peak intensity. So, the weak 2D peak was caused by N doping, the graphene-metal interaction and the multi-walled carbon nanotubes.

The high intensity of C(002) peak in XRD data (Fig 2e, Fig S13d) was ascribed to the in-situ formed some multi-walled carbon nanotubes during the formation of single laye graphene encapsulating metal nanoparticles, as the HRTEM images shown in Fig 2b-c, S1-2.

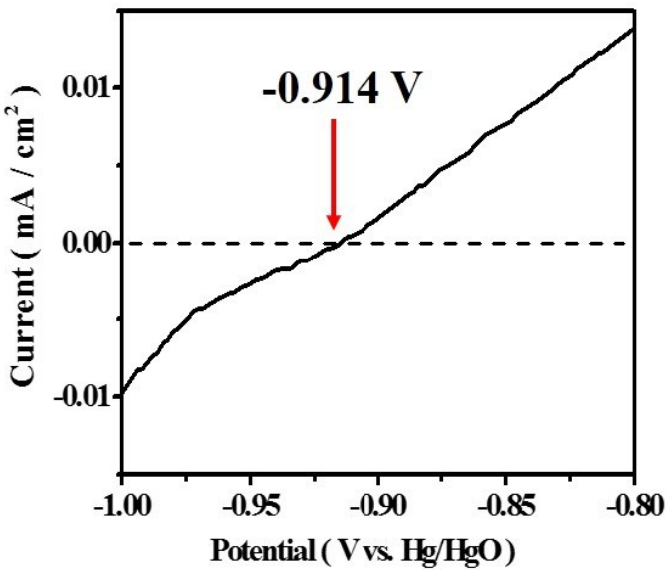

Figure S14. The Hg/HgO reference electrode was calibrated in H_2-saturated 1 M NaOH solution by measuring hydrogen oxidation/evolution at a platinum wire electrode and defining the point of zero current as 0 V versus reversible hydrogen electrode (RHE).

Electrolyte	Reference electrode	Thermodynamic potential for hydrogen electrode	Conversion equation
1 M NaOH	Hg/HgO	-0.914 V vs. Hg/HgO	E(RHE)=E(Hg/HgO)+0.914

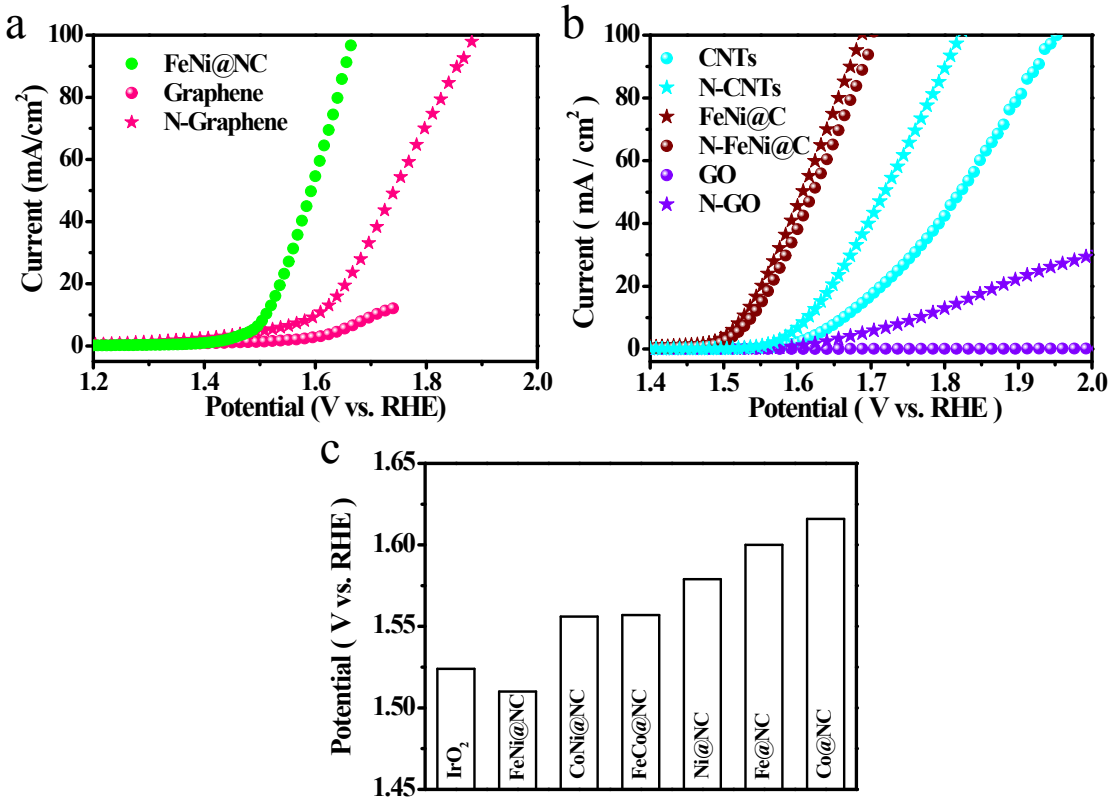

Figure S15. (a-b) OER polarization curves for FeNi@NC in comparison with graphene, N-graphene, FeNi@C, N-FeNi@C, CNTs, N-CNTs, GO and N-GO with same mass loading. **(c)** The overpotential required for M@NCs and IrO_2 at 10 mA cm^{-2}.

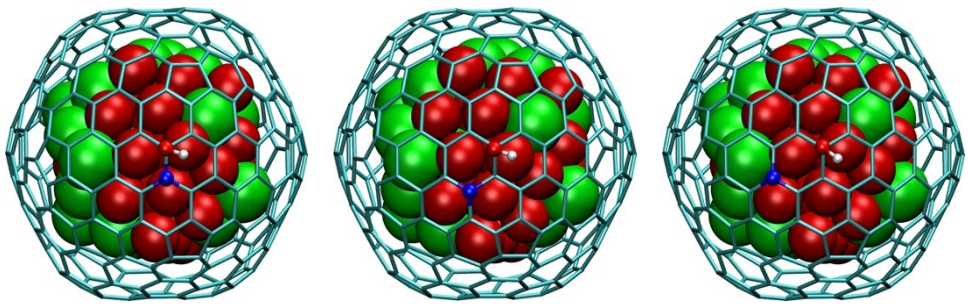

FeNi@NC-1 FeNi@NC-2 FeNi@NC-3

Figure S16. The structures for FeNi@NCs, where large red and green balls represent Fe and Ni, small blue, red and white balls are N, O, H atoms.

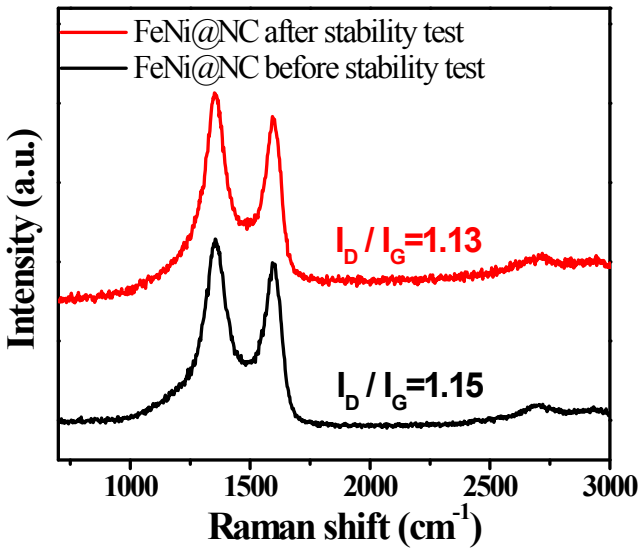

Figure S17. Raman spectra and the corresponding intensity ratio of D peak and G peak (I_D/I_G) of FeNi@NC before and after 5000 cyclic voltammetric (CV) sweeps between -0.46 and 0.54 V (vs. Hg/HgO) at 100 mV s^{-1}. Raman spectroscopy was conducted on a Renishaw instrument with a 532 nm excitation laser. The Raman spectra shows that the FeNi@NC sample possessed a similar degree of graphitization according to the intensity ratio between D and G bands before and after the OER durability tests.

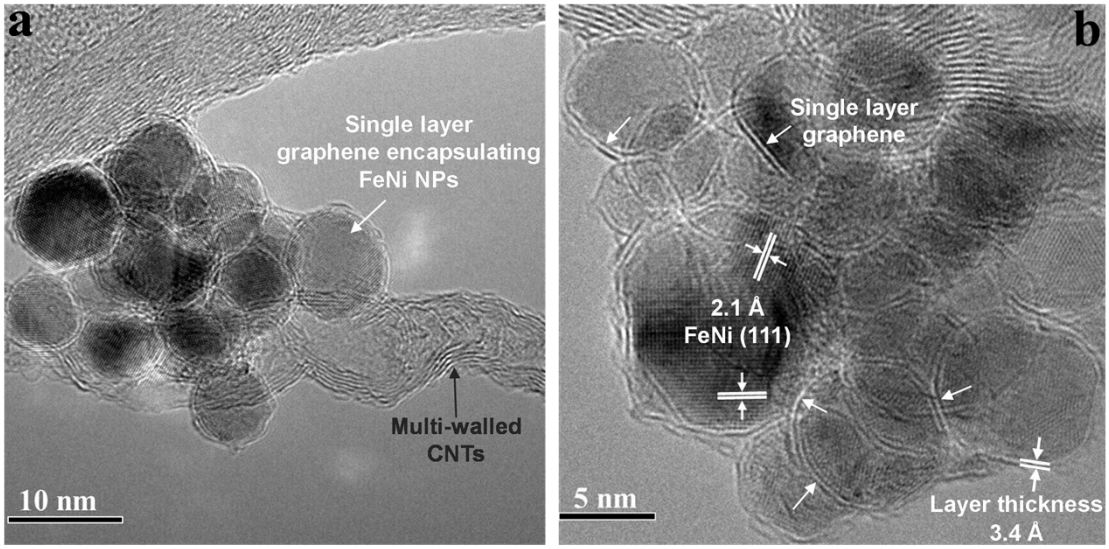

Figure S18. HRTEM images of FeNi@NC after 5000 cyclic voltammetric (CV) sweeps between -0.46 and 0.54 V (vs. Hg/HgO) at 100 mV s^{-1}. The HRTEM images show that the structure of carbon shells encapsulating metal nanoparticles are well maintained after OER durability measurements with 5000 CV sweeps between -0.46 V and +054 V vs. Hg/HgO, and the FeNi nanoparticles exhibit a d spacing of 2.1 Å, in good agreement with the (111) plane of the FeNi alloy.

Table S1. The BET surface area of the prepared electrocatalysts.

sample	**BET surface area (m^2/g)**
Fe@NC	188.3
Co@NC	133.5
Ni@NC	111.6
FeCo@NC	157.1
FeNi@NC	168.2
CoNi@NC	112.1

Table S2. The element compositions of M@NCs estimated from ICP measurements.

Sample	Metal species	Metal (wt %)
Fe@NC	Fe	6.1
Co@NC	Co	34.4
Ni@NC	Ni	32.8
FeCo@NC	Fe	3.4
	Co	3.6
FeNi@NC	Fe	17.7
	Ni	19.1
CoNi@NC	Co	18.2
	Ni	19.8
FeNi@C	Fe	13.2
	Ni	14.4
N-FeNi@C	Fe	4.7
	Ni	5.7

Table S3. The element compositions of M@NCs estimated from Vario EL III measurements.

Sample	C (wt %)	N (wt %)	H (wt %)
Fe@NC	80.1	3.9	0.7
Co@NC	59.2	2.1	0.6
Ni@NC	56.6	4.4	0.5
FeCo@NC	58.2	1.6	0.5
FeNi@NC	67.4	2.9	0.6
CoNi@NC	55.1	1.9	0.6
FeNi@C	69.2	0.1	0.8
N-FeNi@C	84.4	2.1	0.7

Table S4. The element compositions estimated from XPS measurements.

Sample	C (wt %)	N (wt %)	O (wt %)
Fe@NC	83.7	5.6	4.6
Co@NC	59.2	3.0	3.4
Ni@NC	60.5	4.0	2.7
FeCo@NC	84.0	2.8	6.2
FeNi@NC	51.8	3.9	7.5
CoNi@NC	56.3	2.5	3.2
FeNi@C	67.4	-	5.0
N-FeNi@C	83.9	2.7	3.1
N-graphene	90.5	2.8	6.7
CNTs	95.6	-	4.4
N-CNTs	98.7	0.2	1.1
GO	65.5	0.8	33.7
N-GO	86.4	8.7	4.9

Table S5. The electron transfer from encapsulated metals to graphene surface (Q), the free energies for intermediates HO*, O*, HOO* and calculated overpotential (η) for various catalysts. Positive Q for all M@C samples indicates that the electrons transferred from metal to carbon layer enhanced the binding strength of reaction intermediates compared with pure graphene layer.

Sample	**Q** (e^-/metal atom)	**ΔG(HO*)** (eV)	**ΔG(O*)** (eV)	**ΔG(HOO*)** (eV)	**η** (V)
Fe@C	0.15	1.08	2.11	4.31	0.97
Co@C	0.12	0.94	2.0	4.18	0.95
Ni@C	0.07	1.10	2.31	4.29	0.74
FeNi@C	0.10	1.57	3.05	4.77	0.49
Graphene	0	2.34	2.65	5.58	1.7

Table S6. The free energies for intermediates HO*, O*, HOO* and calculated overpotentials (η) for various catalysts.

Sample	ΔG(HO*) (eV)	ΔG(O*) (eV)	ΔG(HOO*) (eV)	η (V)
Carbon	2.34	2.65	5.58	1.70
N-Carbon	0.95	2.31	4.27	0.73
Fe@C	1.08	2.11	4.31	0.97
Fe@NC	1.03	1.96	4.28	1.09
Co@C	0.94	2.0	4.18	0.95
Co@NC	0.92	1.86	4.18	1.10
FeNi@C	1.57	3.05	4.77	0.49
FeNi@NC-1	1.02	1.94	4.22	1.06
FeNi@NC-2	1.22	2.25	4.42	0.94
FeNi@NC-3	1.25	2.57	4.45	0.62

FeNi@NC-1, FeNi@NC-2 and FeNi@NC-3 denote different N-doping sites as shown in Figure S16. In general, N-doping and enclosed metal cluster will synergistically enhance the adsorption for all intermediates as shown in Table S6. However, the overpotentials don't always decrease correspondingly. For pure carbon materials, N-doping can decrease the overpotential from 1.7 V to 0.73 V. In contrast, N-doping will increase the overpotentials for the M@C samples. The reason is that the OER overpotentials don't simply depend on the adsorption energy of O* and HO* but the differences between them. In conclusion, the increase of OER activity for the M@C samples by N-doping in experiment (Figure S15 (b)) should be a compromise of the contribution of N-doped carbon and N-doped graphene encapsulating metal NPs.

Table S7. The potential required for M@NCs at the current density of 2 mA cm^{-2}.

Sample	Fe@NC	Co@NC	Ni@NC	FeNi@NC	CoNi@NC	FeCo@NC
Potential (V)	1.55	1.56	1.50	1.44	1.49	1.51

Table S8. The DFT calculated zero point energy corrections and entropic contributions to the free energies.

Sample	E(eV)	ZPE(eV)	TΔS(eV)
HO*	-	0.35	0
O*	-	0.05	0
HOO*	-	0.41	0
H_2	-6.76	0.27	0.67
H_2O	-14.23	0.56	0.41
O_2	-9.86	0.10	0.64

Table S9. Summary of our catalysts and the representative OER catalysts in literatures .

catalyst	Catalyst amount (mg/cm^2)	Electrolyte solution	Potential at 10 mA/cm^2 (vs. RHE)	reference
FeNi@NC	0.32	1 M NaOH	1.51	This work
IrO_2	0.32	1 M NaOH	1.52	This work
3D g-C_3N_4 NS–CNT	0.20	0.1 M KOH	1.60	[11]
Nitrogen-doped carbon	0.20	KOH (pH =13)	1.61	[12]
Nitrogen-Doped Graphene/Carbon Nanotube Hybrids	0.26	0.1 M KOH	1.63	[13]
$Fe_6Ni_{10}Ox$	0.10	1 M KOH	1.52	[14]
NiFe-LDH NP film on Ni foam	~1.0	0.1 M KOH	1.48	[15]
n NiFe LDH/NGF	0.25	0.1 M KOH	1.57	[16]
IrO_2-CNT	0.20	0.1 M KOH	1.59 V	[11]
NG-NiCo	0.25	1 M KOH	~1.48	[17]
Co_3O_4/N-graphene	0.24	0.1 M KOH	1.60	[18]
Co_3O_4/SWNTs	0.05	1 M KOH	1.80	[19]
FeNi-rGO LDH	0.25	1 M KOH	1.44	[20]
Fe@N – C-700	0.32	0.1 M KOH	1.70	[21]
Co@N – C	4.5	1 M KOH	1.60	[22]
3D Ni foam/porous carbon/anodized Ni	[a]	0.1 M KOH	1.75	[23]
ECPT-Co@C	0.04	1 M KOH	1.60	[24]
FeNi nanosheets	0.07	1 M KOH	1.53	[25]
$(Pr_{0.5}Ba_{0.5})CoO_{3-\delta}$	0.25	0.1 M KOH	1.56	[26]

[a] The catalyst amount was not given in the reference.

References

1. D. H. Deng, L. Yu, X. L. Pan, S. Wang, X. Q. Chen, P. Hu, L. X. Sun and X. H. Bao, *Chem Commun*, 2011, **47**, 10016-10018.
2. G. Kresse and J. Hafner, *Phys. Rev. B*, 1993, **47**, 558-561.
3. G. Kresse and J. Hafner, *Phys. Rev. B*, 1994, **49**, 14251-14269.
4. A. Taniguchi, M. Fukushima, M. Sakai, K. Kataoka, I. Nagata, K. Doi, H. Arakawa, S. Nagasaka, K. Tokuyama and Y. Nakai, *Metabolism*, 2000, **49**, 1001-1005.
5. H. Arakawa, H. Kodama, I. Yamaguchi and N. Matsuoka, *Pharmacol Biochem Be*, 2000, **66**, 707-712.
6. X. L. Pan, Z. L. Fan, W. Chen, Y. J. Ding, H. Y. Luo and X. H. Bao, *Nat Mater*, 2007, **6**, 507-511.
7. W. Chen, X. L. Pan, M. G. Willinger, D. S. Su and X. H. Bao, *J. Am. Chem. Soc*, 2006, **128**, 3136-3137.
8. W. Chen, X. L. Pan and X. H. Bao, *J. Am. Chem. Soc*, 2007, **129**, 7421-7426.
9. P. E. Blöchl, *Phys. Rev. B*, 1994, **50**, 17953-17979.
10. I. C. Man, H. Y. Su, C. V. Federico, H. A. Hansen, J. I. Martínez, N. G. Inoglu, K. John, T. F. Jaramillo, J. K. Nørskov and R. Jan, *Chem. Cat. Chem.*, 2011, **3**, 1159-1165.
11. T. Y. Ma, S. Dai, M. Jaroniec and S. Z. Qiao, *Angew. Chem. Int. Ed.*, 2014, **53**, 7281-7285.
12. Y. Zhao, R. Nakamura, K. Kamiya, S. Nakanishi and K. Hashimoto, *Nat. Commun.*, 2013, **4**, 2390.
13. G. L. Tian, M. Q. Zhao, D. Yu, X. Y. Kong, J. Q. Huang, Q. Zhang and F. Wei, *Small*, 2014, **10**, 2251-2259.
14. L. Kuai, J. Geng, C. Y. Chen, E. J. Kan, Y. D. Liu, Q. Wang and B. Y. Geng, *Angew. Chem. Int. Ed.*, 2014, **53**, 7547-7551.
15. Z. Lu, W. Xu, W. Zhu, Q. Yang, X. Lei, J. Liu, Y. Li, X. Sun and X. Duan, *Chem. Commun.*, 2014, **50**, 6479-6482.
16. C. Tang, H. S. Wang, H. F. Wang, Q. Zhang, G. L. Tian, J. Q. Nie and F. Wei, *Adv Mater*, 2015, **27**, 4516-4522.
17. S. Chen, J. J. Duan, M. Jaroniec and S. Z. Qiao, *Angew. Chem. Int. Ed.*, 2013, **52**, 13567-13570.
18. Y. Y. Liang, Y. G. Li, H. L. Wang, J. G. Zhou, J. Wang, T. Regier and H. J. Dai, *Nat. Mater.*, 2011, **10**, 780-786.
19. J. Wu, Y. Xue, X. Yan, W. Yan, Q. Cheng and Y. Xie, *Nano Res.*, 2012, **5**, 521-530.
20. X. Long, J. K. Li, S. Xiao, K. Y. Yan, Z. L. Wang, H. N. Chen and S. H. Yang, *Angew. Chem. Int. Ed.*, 2014, **53**, 7584-7588.
21. J. Wang, H. Wu, D. Gao, S. Miao, G. Wang and X. Bao, *Nano Energy*, 2015, **13**, 387-396.
22. J. Wang, D. Gao, G. Wang, S. Miao, H. Wu, J. Li and X. Bao, *J. Mater. Chem. A*, 2014, **2**, 20067-20074.
23. J. Wang, H. X. Zhong, Y. L. Qin and X. B. Zhang, *Angew. Chem. Int. Ed.*, 2013, **52**, 5248-5253.
24. Q. Xiao, Y. Zhang, X. Guo, L. Jing, Z. Yang, Y. Xue, Y. M. Yan and K. Sun, *Chem. Commun.*, 2014, **50**, 13019-13022.

25. F. Song and X. Hu, *Nat. Commun.*, 2014, **5**, 4477.
26. A. Grimaud, K. J. May, C. E. Carlton, Y. L. Lee, M. Risch, W. T. Hong, J. Zhou and Y. Shao-Horn, *Nat. Commun.*, 2013, **4**, 2439.